Fixed-angle plate fixation in simulated fractures of the proximal humerus: A biomechanical study of a new device

Steven C. Chudik, MD,[a] Paul Weinhold, PhD,[b] and Laurence E. Dahners, MD,[b] *Hinsdale, IL, and Chapel Hill, NC*

This study was performed to evaluate the biomechanical properties of a new device for displaced fractures of the proximal humerus. The device is a low-profile, fixed-angle plate specially designed for percutaneous application. With the use of embalmed cadaveric humeri, we simulated both noncomminuted and comminuted 2-part surgical neck fractures of the proximal humerus. Each humerus of a pair was then randomly fixed with either the new experimental device or the Association for the Study of Internal Fixation (ASIF) T-plate and mechanically tested to failure in an axial shear-loading model. The two fixation devices were evaluated in paired humeri with regard to mode of failure, stiffness, displacement at physiologic loads, and displacement, load, and energy at the point of ultimate load before failure. In the noncomminuted fracture trials the experimental device exhibited significantly greater stiffness ($P < .001$; $P = .002$ for normalized values) and ultimate load before failure ($P = .015$) and significantly less displacement at higher physiologic loads ($P = .031$). In the comminuted fracture trials the experimental device exhibited significantly greater stiffness ($P = .048$), ultimate load ($P < .001$) and energy absorbed ($P = .048$) before failure, and significantly less displacement at higher ($P = .004$) and lower physiologic loads ($P = .011$). The study demonstrates improved biomechanical properties for the new experimental device over the T-plate in simulated fractures of the proximal humerus. We extrapolate that these improved biomechanical properties may prove advantageous in future clinical investigation. (J Shoulder Elbow Surg 2003;12:578-88.)

From Hinsdale Orthopaedic Associates,[a] Hinsdale, and University of North Carolina, Department of Orthopaedic Surgery,[b] Chapel Hill.

This study received funding from the Aileen Stock Orthopaedic Research Fund and University of North Carolina Department of Orthopaedics, Chapel Hill, NC.

Reprint requests: Steven C. Chudik, MD, 550 W Ogden, Hinsdale, IL 60521 (E-mail: *chudiks@hoasc.com*).

1058-2746/2003/$35.00 + 0
doi:10.1016/S1058-2746(03)00217-9

Numerous devices for fixation of displaced proximal humerus fractures have been described in the literature.* The most common devices include plate fixation, fixed-angle plate fixation, antegrade intramedullary fixation, tension-band wiring, percutaneous fixation, and external fixation. These devices are not entirely without limitation, and we believe that a more optimal device potentially remains to be discovered.

Through evaluating the strengths and weaknesses of these devices, we attempted to design a novel device and technique. Our efforts resulted in a percutaneously applied, low-profile, fixed-angle plate with means to secure tuberosity fragments with tension-band suture (Figures 1 and 2). The fixed-angle plate design utilizes the greater stiffness and load to failure reported with plate fixation in previous cadaveric biomechanical studies.[3,11,13,27,28] Percutaneous application allows rapid insertion as with antegrade intramedullary, percutaneous fixation, and external fixation devices and minimizes the dissection and increased rates of avascular necrosis associated with standard open plate application.[6,29] Its low profile on the greater tuberosity avoids impingement with the acromion, which has been reported with other plates,[6,15,24] antegrade intramedullary devices,[7,31] antegrade percutaneous fixation, and external fixation.[12,16] Tension banding through special proximal holes in the plate will allow for secure fixation of the tuberosity fragments, a feature greatly lacking with many other common devices. Lastly, the device is equipped with proximally directed fixed-angle (130°) screws that follow the consistent shaft-head angle of the proximal humerus and allow for superior fixation in the center of the humeral head.[1,17]

To evaluate this new device, we undertook a biomechanical cadaveric study to compare the stiffness, displacement at physiologic loads, and displacement, load, and energy absorbed at the point of ultimate load before failure of this new device against previous standards. Through a biomechanical comparison of 10 different fixation devices, Koval et al[13] established the Association for the Study of Internal Fixation (ASIF) T-plate as a standard against which

*References 2, 4-6, 9, 12-14, 16, 19, 20, 26, 28, 30, 31, 33.

Figure 1 The experimental device is specially contoured to fit both left and right humeri. The small proximal holes are used for wires or sutures to secure tuberosity fragments or to reinforce the fixation of surgical neck fractures in a tension band–like configuration through the rotator cuff. The second set of proximal holes is designed to direct three 4.5-mm partially threaded screws at a fixed angle of 130° safely beneath the axillary nerve and into the center of the humeral head. The distal three holes are designed to capture three 4.5-mm large fragment bicortical screws.

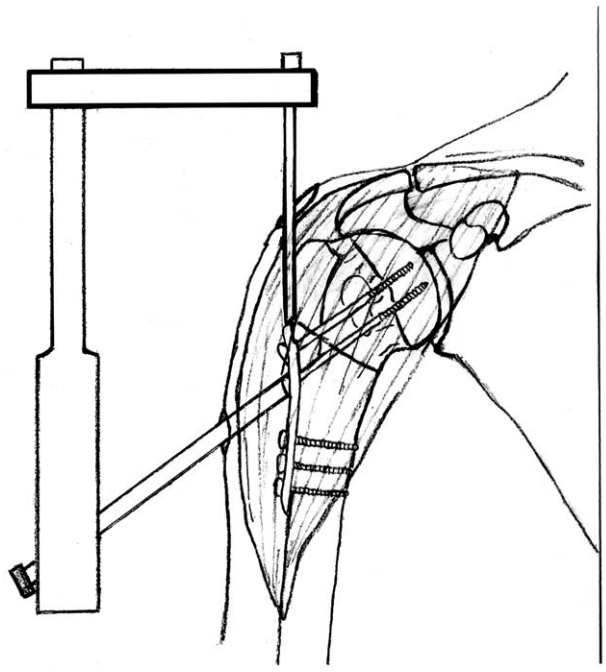

Figure 2 Percutaneous application through a small deltoid-splitting approach.

other devices for fixation of the proximal humerus can be compared. The ASIF T-plate was found to exhibit superior in vitro biomechanical properties in other studies as well.[3,28] Using a protocol similar to that of Koval et al, we tested our hypothesis that this new device would provide at least equivalent biomechanical properties to that of the ASIF T-plate.

MATERIALS AND METHODS

Specimen preparation

Twenty-four pairs of humeri were harvested from embalmed cadavers, stripped of all of their adherent soft tissues, and used for study. The mean age of the cadavers was 77.6 years, with a range of 50 to 97 years. All cadavers were screened for cause of death, and their humeri were grossly inspected for deformity. Humeri with evidence of potential alteration of the normal bony architecture by either gross fracture, tumor, or history of malignancy were excluded. The distal humeral condyles were removed, and the humeral shafts were potted with a polyester resin cement (Bondo All-Purpose Putty; Dynatron/Bondo Corporation, Atlanta, GA) in 1-inch–internal diameter polyvinyl chloride piping. Until testing, all humeri were stored as pairs in sealed bags at −20°C.

Preloading

Before the actual experimental testing, the intact potted humeri were axially preloaded to 750 N in our testing model (see "Testing protocol" section) with the use of a servohydraulic materials testing machine (Model 812; MTS Systems Corporation, Minneapolis, MN). Through preloading, we generated load-displacement curves and determined the stiffness of the intact bone from the initial slope. These values were then used to normalize the experimental values for stiffness for each specimen and to eliminate the variability resulting from differences in side-to-side bone quality.

Fracture simulation

In 14 pairs of humeri, we simulated a simple and reproducible noncomminuted 10°, oblique, surgical neck fracture (type 11-A3)[23] by using a band saw with a 0.55-mm-thick blade. The simulated fractures were carefully performed to reproduce the pattern of surgical neck fracture previously described in the literature.[8,22] In another 10 pairs of humeri, we created a 10°, oblique, surgical neck fracture and removed a 1-cm medially based wedge of cortex at the fracture site to represent a comminuted fracture pattern.

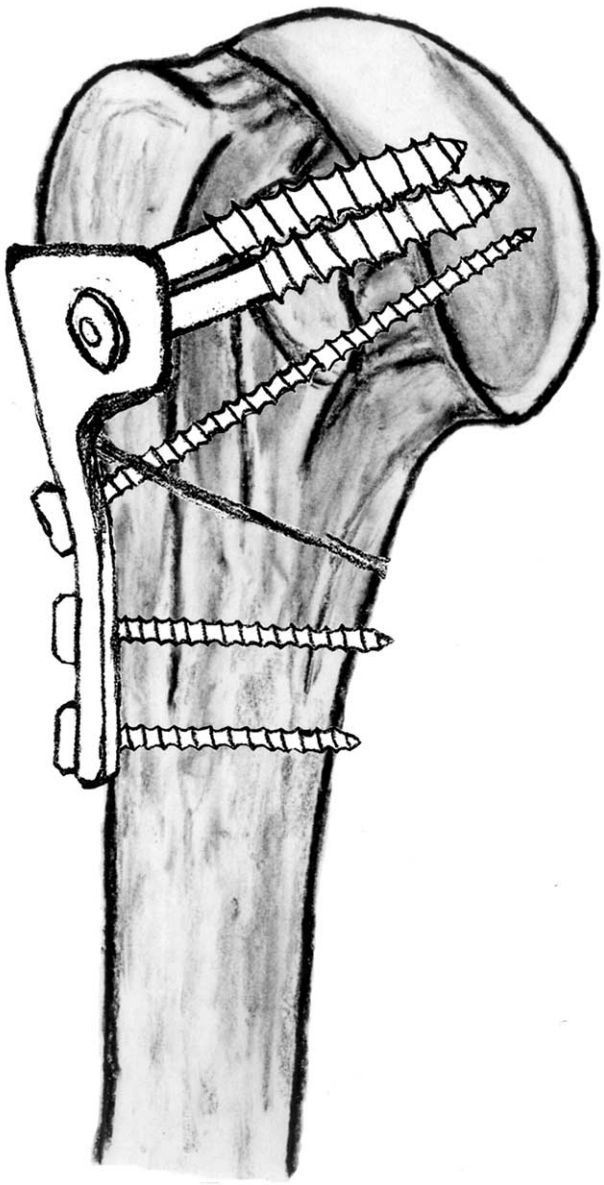

Figure 3 ASIF T-plate.

Fracture fixation

For each pair of humeri, the ASIF T-plate (Synthes, Paoli, PA) and the experimental device were assigned randomly and equally to the right and left specimens to control for side-to-side differences between dominant and nondominant extremities. This was done by random selection from a pool of sealed envelopes in which half of the envelopes indicated experimental fixation for the right side and half indicated the left side. As described by Koval et al,[13] ASIF T-plate fixation was performed with the use of the ASIF 5-hole T-plate with two proximal 6.5-mm partially threaded, cancellous screws, a 4.5-mm cortical lag screw placed from distal to proximal across the fracture site, and two distal 4.5-mm bicortical screws (Figure 3). The new experimental device was placed so that the proximal screws were directed into the center of the humeral head. This consistently left the experimental device just lateral to the bicipital groove with the top of the plate approximately at the level of the inferior edge and the medial humeral articular surface well below the usual site of impingement on the greater tuberosity. The experimental device was fixed with three proximal 4.5-mm partially threaded screws and three distal 4.5-mm bicortical screws (Figure 4). Because the instrumentation for percutaneous insertion was not yet available and there was not adequate rotator cuff tissue on the cadaveric specimen, the new fixation device was applied directly to the bone and the effects of percutaneous application and additional tension-band wiring/suturing were not evaluated by this study.

Testing protocol

Following the testing protocol established by Koval et al,[13] all of the humerus/device constructs were loaded by a uniaxial servohydraulic materials testing machine (Model 812; MTS Systems Corporation) with the humeral shaft oriented at 20° of abduction from vertical to produce primarily axial and shear loading of the fixation (Figure 5). This model closely reproduces the longitudinal direction of force encountered at the geometrical center of the humeral head seen with early active abduction.[10,25] The humeri were continuously loaded to failure at a rate of 10 cm/min. Failure was defined as a marked decrease or discontinuity in the load-displacement curve or greater than 1 cm of displacement.

Data and statistical analysis

After testing, the humerus/device constructs were systematically inspected and sectioned to determine the mode of failure. Load-displacement curves were obtained for each construct, and the values for stiffness, displacement at physiologic loads, and displacement, load, and energy at the point of ultimate load before failure were determined for both methods of fixation. Stiffness was determined from the slope of the linear portion of the load-displacement curve. The stiffness ratio was calculated by dividing the stiffness of the fractured humerus/implant construct by the value of stiffness determined from the previous preloading of the respective intact humerus. Physiologic loads were estimated from the work of Poppen and Walker.[25] We chose to evaluate displacement at loads of 0.3 kN and 0.6 kN, which represent the forces seen at articular surface of the humerus acting with an orientation through the geometrical center of the humerus when the arm is actively held in a position of 30° abduction and 90° abduction, respectively. Paired and unpaired Student t tests were used to evaluate for differences due to fixation methods and comminution, respectively.

RESULTS

Observed mode of failure

In the noncomminuted fracture trials, 5 particularly large matched specimens with good bone quality (fixed with the experimental device and the T-plate)

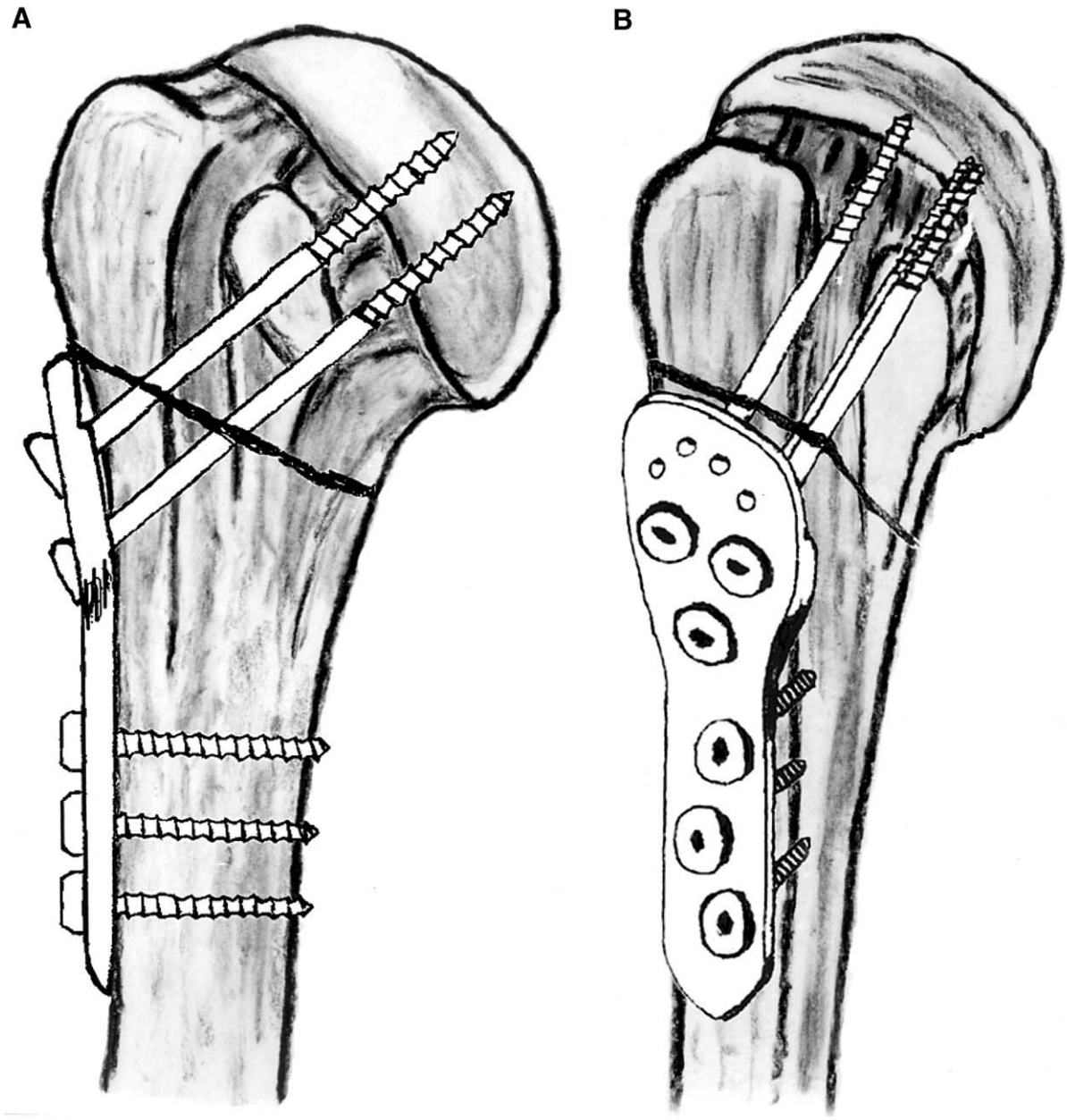

Figure 4 Experimental device: Anteroposterior (**A**) and lateral (**B**) views.

failed away from the simulated fracture site, leaving the device/fracture construct intact. This mode of failure allowed us to determine accurately the stiffness and displacement at physiologic loads for these 5 specimens but precluded measurement of the variables dependent on failure of the construct (ie, displacement, ultimate load, and energy absorption at the point of ultimate load before failure).

For the rest of the noncomminuted trials, the specimens fixed with the T-plate yielded quickly in response to load. The proximal screws pulled out of the head, resulting in varus angulation and proximal medial cortical failure of the distal fragment. At the completion of the test, the T-plate/noncomminuted fracture constructs were significantly weakened by the loss of proximal fixation and bony disruption and were easily disassembled by manipulation. The noncomminuted specimens fixed with the experimental device resisted displacement and angulation initially and eventually failed by impaction and shear at the fracture site, with minimal varus angulation as the proximal end of the screws cut (less than a few

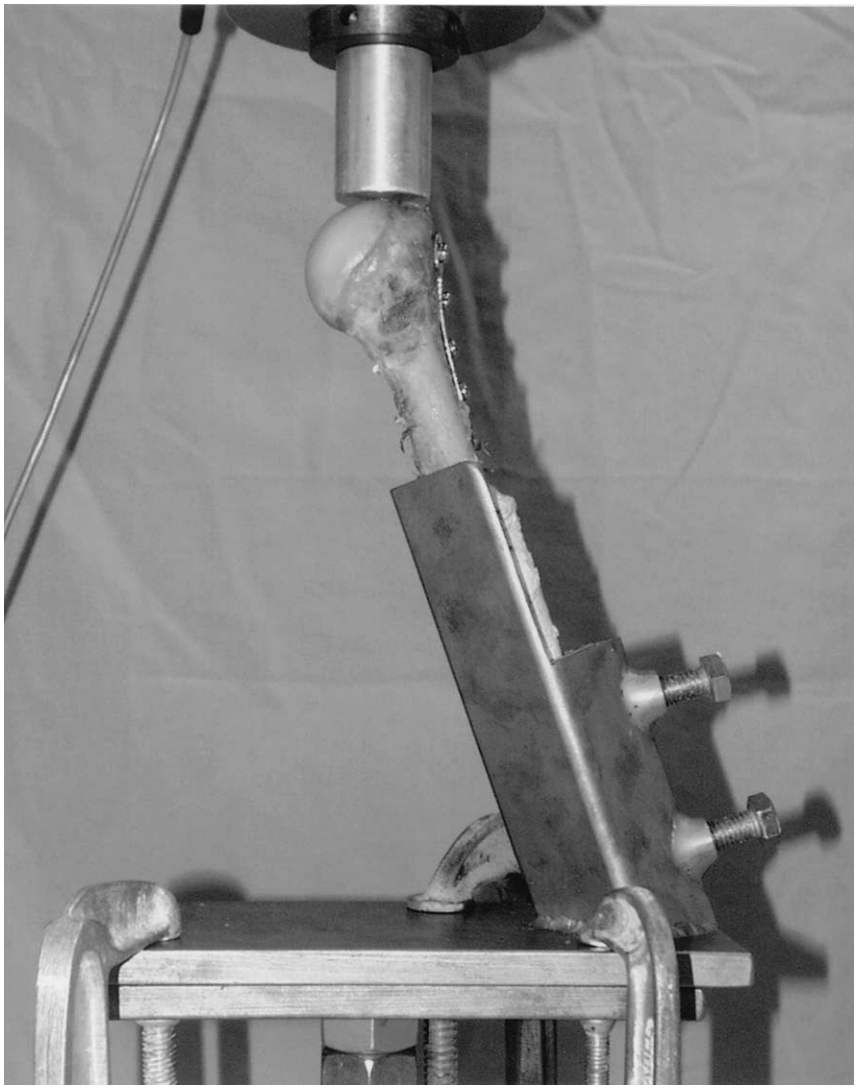

Figure 5 Testing model.

millimeters) through the cancellous bone at the distal end of the proximal fragment (head). At the completion of the test, the experimental device/noncomminuted fracture constructs often remained intact and were difficult to disassemble by manipulation.

As opposed to the noncomminuted trials, all of the specimens in the comminuted trials failed at the simulated fracture site. The comminuted specimens fixed with the T-plate yielded immediately as the load was applied, resulting in varus angulation, closure of the medial cortical defect, and different degrees of proximal screw pullout. At the completion of the test, the T-plate/comminuted fracture constructs were significantly weakened by loss of proximal fixation and were easily disassembled by manipulation. The comminuted specimens fixed with the experimental device resisted displacement, angulation, and closure of the medial bony defect. Similar to the noncomminuted specimens, they failed by impaction and shear at the fracture site, with minimal varus angulation as the proximal end of the screws cut through the cancellous bone at the distal end of the proximal fragment (head). Despite the additional bony deficiency, the experimental device/comminuted fracture constructs often remained intact and were difficult to disassemble by manipulation.

Differences in biomechanical parameters between experimental device and T-plate

For the biomechanical parameters measured, we found significant differences between the ASIF T-plate and the experimental device (Tables I and II). In the noncomminuted trials the experimental device exhib-

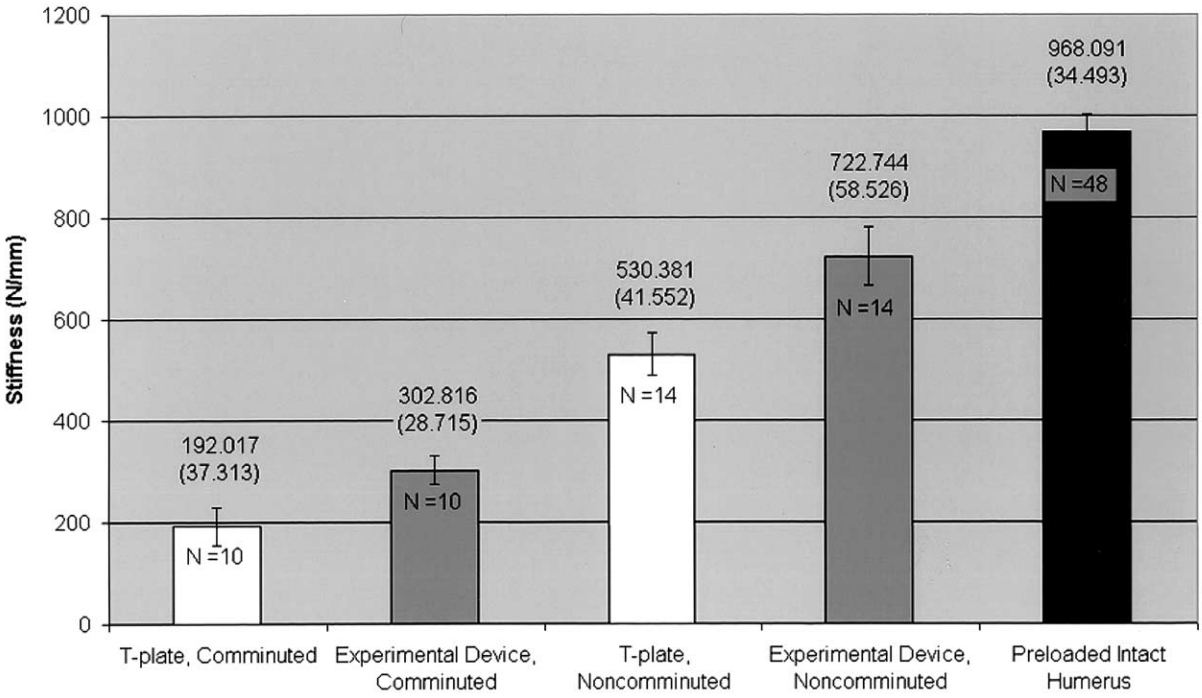

Figure 6 Stiffness: Experimental device versus T-plate for comminuted and noncomminuted trials. Data are presented as mean (SE). *N*, Sample size.

Table I Experimental device versus T-plate: Noncomminuted trials

	Stiffness (N/mm)	Stiffness ratio: Fracture/ intact	Displacement at 0.3 kN (mm)	Displacement at 0.6 kN (mm)	Displacement before failure (mm)	Ultimate load before failure (kN)	Energy before failure (J)
Experimental device [mean (SE)]	722.744 (58.526)	0.721 (0.031)	0.611 (0.088)	1.091 (0.116)	6.022 (0.582)	2.299 (0.232)	8.655 (1.524)
T-plate [mean (SE)]	530.381 (41.552)	0.552 (0.046)	0.718 (0.081)	1.536 (0.258)	5.033 (0.586)	1.876 (0.221)	5.645 (1.204)
Difference	192.363	0.169	–0.107	–0.446	0.989	0.422	3.010
Sample size	14	14	14	14	9	9	9
P value	<.001	.002	.242	.031	.192	.015	.071

Table II Experimental device versus T-plate Comminuted trials

	Stiffness (N/mm)	Stiffness ratio: Fracture/ intact	Displacement at 0.3 kN (mm)	Displacement at 0.6 kN (mm)	Displacement before failure (mm)	Ultimate load before failure (kN)	Energy before failure (J)
Experimental device [mean (SE)]	302.816 (28.715)	0.316 (0.023)	1.128 (0.184)	2.976 (0.530)	8.450 (0.482)	1.458 (0.146)	8.543 (1.056)
T-plate [mean (SE)]	192.017 (37.313)	0.224 (0.036)	2.603 (0.394)	5.137 (0.955)	8.922 (0.643)	1.190 (0.139)	6.556 (1.039)
Difference	110.799	0.0922	–1.475	–2.161	–0.473	0.268	1.988
Sample size	10	10	10	10	10	10	10
P value	.048	.102	.004	.011	.467	<.001	.048

ited significantly higher values for absolute stiffness, the stiffness ratio (fractured/preloaded value), and ultimate load before failure (Figures 6 and 7). The experimental device also exhibited significantly less displacement at higher physiologic loads of 0.6 kN (Figure 8). There was a trend for the experimental

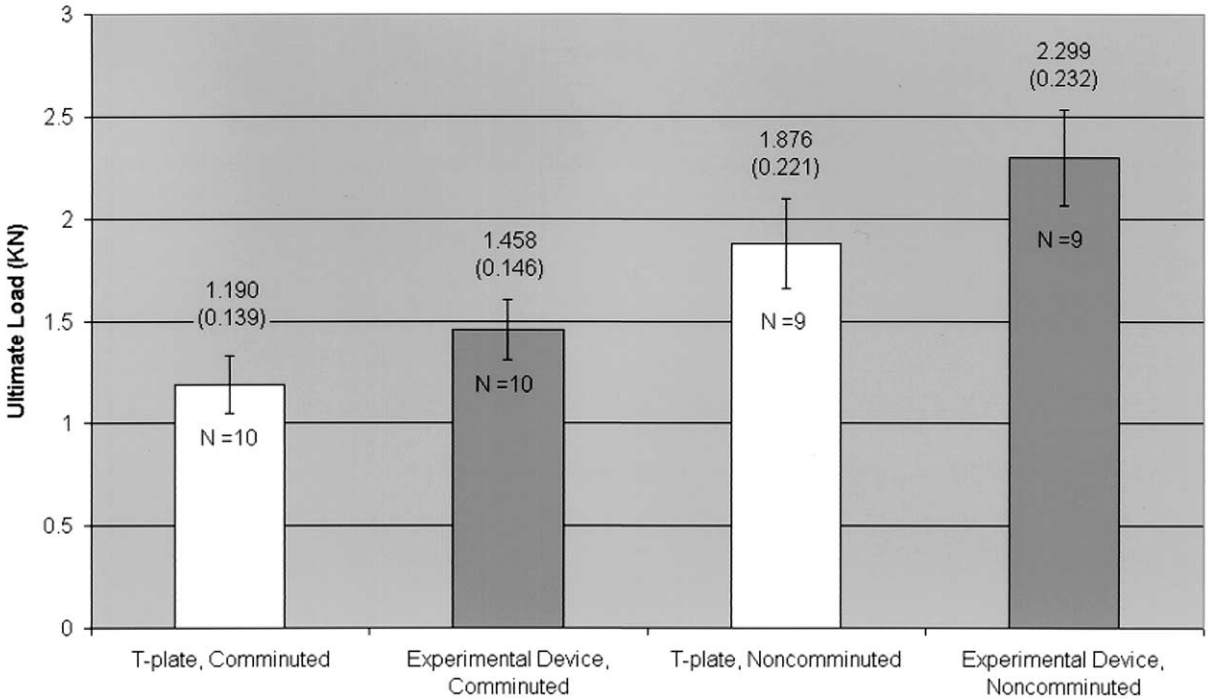

Figure 7 Ultimate load before failure: Experimental device versus T-plate for comminuted and noncomminuted trials. Data are presented as mean (SE). *N*, Sample size.

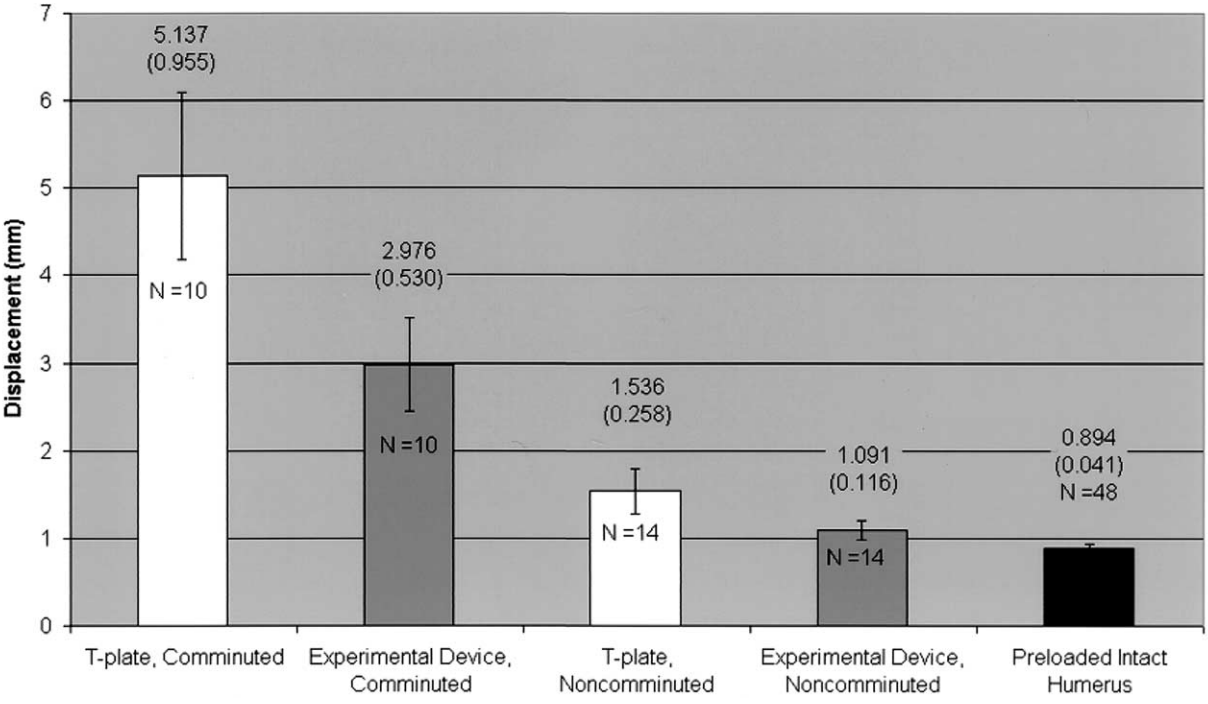

Figure 8 Displacement at higher physiologic load (0.6 kN): Experimental device versus T-plate for comminuted and noncomminuted trials. Data are presented as mean (SE). *N*, Sample size.

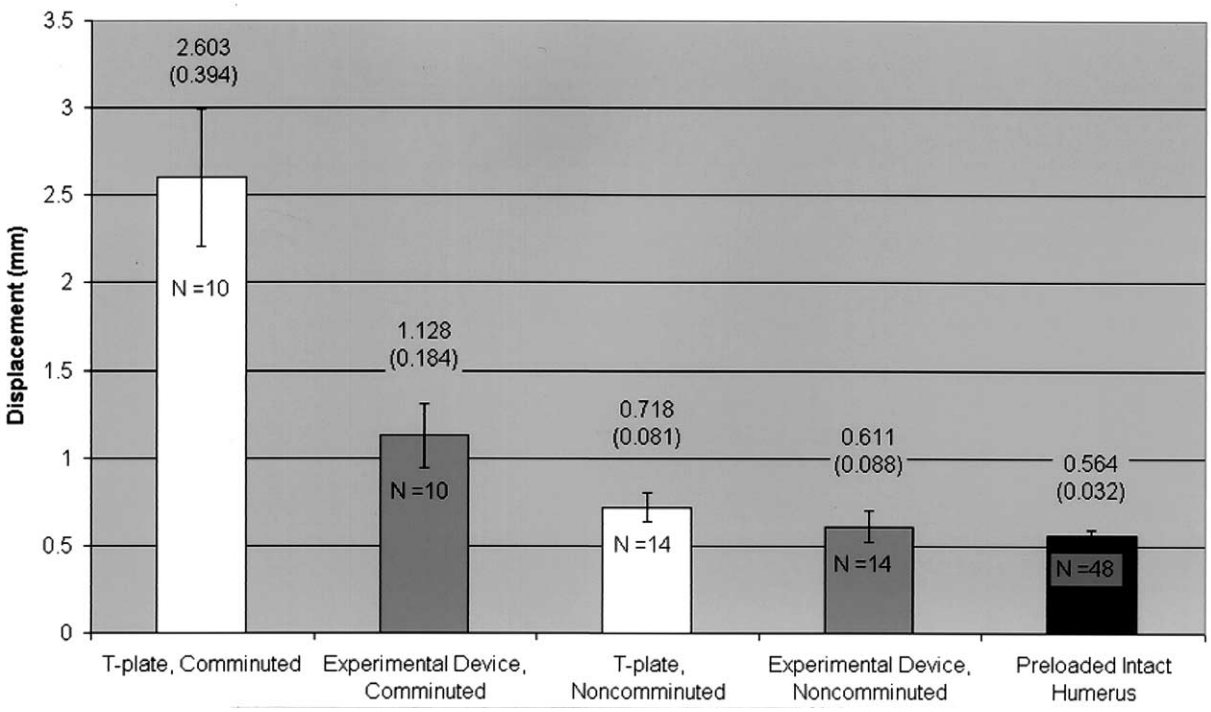

Figure 9 Displacement at lower physiologic load (0.3 kN): Experimental device versus T-plate for comminuted and noncomminuted trials. Data are presented as mean (SE). *N*, Sample size.

Table III Noncomminuted versus comminuted trials: Experimental device

	Stiffness (N/mm)	Stiffness ratio: Fracture/intact	Displacement at 0.3 kN (mm)	Displacement at 0.6 kN (mm)	Displacement before failure (mm)	Ultimate load before failure (kN)	Energy before failure (J)
Noncomminuted [mean (SE)]	722.744 (58.526)	0.721 (0.031)	0.611 (0.088)	1.091 (0.116)	5.891 (0.423)	2.218 (0.185)	8.497 (1.197)
Comminuted [mean (SE)]	192.017 (28.715)	0.316 (0.023)	1.128 (0.184)	2.976 (0.530)	8.450 (0.482)	1.458 (0.146)	8.543 (1.056)
Difference	419.928	0.406	–0.517	–1.886	–2.559	0.760	0.046
Sample size	14 NC 10 Com	14 NC 10 Com	14 NC 10 Com	14 NC 10 Com	14 NC 10 Com	14 NC 10 Com	14 NC 10 Com
P value	<.001	<.001	.011	<.001	<.001	.006	.979

NC, Noncomminuted; *Com,* comminuted.

Table IV Noncomminuted versus comminuted trials: T-plate

	Stiffness (N/mm)	Stiffness ratio: Fracture/intact	Displacement at 0.3 kN (mm)	Displacement at 0.6 kN (mm)	Displacement before failure (mm)	Ultimate load before failure (kN)	Energy before failure (J)
Noncomminuted [mean (SE)]	530.381 (41.552)	0.552 (0.046)	0.718 (0.081)	1.536 (0.258)	5.199 (0.501)	1.985 (0.199)	6.795 (1.114)
Comminuted [mean (SE)]	192.017 (37.313)	0.224 (0.036)	2.603 (0.394)	5.137 (0.955)	8.922 (0.643)	1.190 (0.139)	6.556 (1.039)
Difference	338.364	0.329	–1.885	–3.601	–3.724	0.795	0.240
Sample size	14 NC 10 Com	14 NC 10 Com	14 NC 10 Com	14 NC 10 Com	14 NC 10 Com	14 NC 10 Com	14 NC 10 Com
P value	<.001	<.001	<.001	<.001	<.001	.006	.881

NC, Noncomminuted; *Com,* comminuted.

device to allow for more energy absorption before failure.

In the comminuted trials the experimental device exhibited significantly higher values for absolute stiffness and ultimate load and energy absorbed before failure (Figures 6 and 7). The experimental device also exhibited significantly less displacement at lower physiologic loads (0.3 kN) and at higher physiologic loads (0.6 kN) (Figures 8 and 9). There was a trend for the experimental device to exhibit a higher stiffness ratio.

Differences in biomechanical parameters between noncomminuted and comminuted trials

We also found significant differences in biomechanical parameters between the comminuted and noncomminuted trials for both the experimental device and the T-plate (Tables III and IV). Relative to the noncomminuted trials, the comminuted specimens exhibited significantly lower values for stiffness, the stiffness ratio, and ultimate load before failure. The comminuted specimens exhibited significantly higher values for displacement at lower physiologic loads (0.3 kN), at higher physiologic loads (0.6 kN), and at the point of ultimate load before failure. There were no significant differences in the amount of energy absorbed before failure between the noncomminuted and comminuted trials.

DISCUSSION

For our investigation, we chose the T-plate as the standard against which to compare our experimental device. Despite its known clinical limitations, the T-plate has been defined as an appropriate standard for comparison by its superior performance and universal application in several previous in vitro biomechanical studies.[11,13,21,27,28,32] Relative to the T-plate, the experimental device exhibited significantly greater stiffness and ultimate load before failure and significantly less displacement at higher physiologic loads (0.6 kN) for noncomminuted specimens. In the comminuted trials the experimental device exhibited significantly greater stiffness and ultimate load and energy absorbed before failure and significantly less displacement at physiologic loads (0.3 kN and 0.6 kN).

With regard to the mode of failure, we observed differences between the two methods of fixation that potentially explain their differences in biomechanical performance. Both methods of fixation failed proximally in the head fragment, and the distal fixation to the shaft was not noticeably affected. From this observation, we postulate that the differences in the proximal design between the experimental device and the T-plate most likely account for the measured and observed differences in biomechanical performance. Specifically, we believe that the proximal fixed-angle screws of the experimental device that are directed into the center of the humeral head are most likely responsible for the differences. The fixed-angle design should provide more resistance to angulation, and the center of the humeral head has been shown to provide increased trabecular bone density, greater length for screw purchase, and superior screw pullout strength.[17]

The observed differences in the mode of failure may also suggest a theoretical clinical benefit for the experimental device. We observed that the T-plate construct yielded more quickly as it fell into varus malalignment. Its proximal fixation loosened, and the structural integrity of the construct was grossly disrupted. On the other hand, the experimental device resisted displacement and angulation, and the construct remained intact on completion of the test. By extrapolation from these in vitro observations, the experimental device may be able to withstand a single high loading event, such as a fall or forceful muscular contraction, better in the early postoperative period and may maintain sufficient alignment and integrity to go on to uncomplicated union.

Differences measured in displacement at physiologic loads may also pose some clinical relevance. In the noncomminuted trials at lower physiologic loads (0.3 kN), there was no significant difference in displacement between the two methods of fixation, suggesting that there may be no advantage to either method of fixation in patients with simple noncomminuted fractures who can comply with a well-supervised postoperative rehabilitation protocol. However, in the noncomminuted trials at higher physiologic loads (0.6 kN) and in the comminuted trials at both lower and higher physiologic loads (0.3 kN and 0.6 kN), the experimental device exhibited significantly less displacement, suggesting that there may be a theoretical advantage to using the experimental device in patients with comminuted fractures and also in patients with noncomminuted fractures who may have difficulty complying with postoperative activity limitations.

The differences in the measured and observed biomechanical properties between the noncomminuted and comminuted trials reveal the obvious and significant role that fracture configuration plays in the fixation of proximal humerus fractures. The comminuted specimens, whether fixed with the experimental device or the T-plate, exhibited significantly less stiffness and ultimate load before failure and significantly higher values for displacement at physiologic loads.

Despite showing a statistically significant difference between the standard ASIF T-plate and the experimental device, this biomechanical study still has many limitations. The major ones include the simu-

lated fractures, the embalmed specimens, and the simple loading pattern of the constructs. Because proximal humerus fractures tend to occur in osteoporotic bone, these clean osteotomies do not fully represent the actual properties of a fracture in vivo. Our attempt to simulate comminution may have helped to recreate a more realistic fracture pattern, but the obvious requirement for reproducibility between specimens prevents us from producing the unique and complex fracture patterns seen in vivo.

Embalming techniques do alter the mechanical properties of bone, but the embalmed specimens used for this study most likely only underestimated the compressive mechanical properties of the humerus. Embalming has been shown to decrease the compressive strength of cortical bone by McElhaney et al,[18] and Koval et al,[13] using the same testing model, reported that for any given method of proximal humerus fixation, embalmed specimens performed biomechanically inferiorly to fresh-frozen specimens.

The simple loading pattern used in our study is unlikely to reproduce the actual complex assortment of forces and factors encountered in vivo. Our model fails to account for torsional forces, forces in the sagittal plane, multidirectional forces, cyclic loading, and bone healing. For this initial investigation, we chose to perform our biomechanical assessment with the use of a previous loading model for comparison that does roughly approximate the longitudinal direction of forces seen at the glenohumeral joint with early shoulder abduction.[25] The mode of failure observed in our T-plate trials is very similar to that previously described in in vivo clinical trials, providing some validation for our loading model.[6,15,24]

In conclusion, this new experimental device possesses many theoretical design advantages over the previous methods of fixation described for the treatment of displaced fractures of the proximal humerus. With the use of a limited cadaveric model, we were able to demonstrate improvements in biomechanical properties relative to the ASIF T-plate, an appropriate in vitro standard for comparison. Future studies will be required to evaluate the proposed theoretical advantages and safety of this new experimental device. In particular, studies will be required to investigate its percutaneous application with regard to the risk for axillary nerve injury and the adequacy of fracture reduction and construct stability.

We would like to thank the University of North Carolina Medical Scientist Training Laboratory for providing the cadaveric specimens, Synthes (Paoli, PA) for manufacturing the experimental device to our specifications and design, and the University of North Carolina Physics Shop for building our jigs for testing and making some necessary modifications to the manufactured device.

REFERENCES

1. Boileau P, Walch G. The three-dimensional geometry of the proximal humerus: implications for surgical technique and prosthetic design. J Bone Joint Surg Br 1997;79:857-65.
2. Bosworth DM. Blade plate fixation: technic suitable for fractures of the surgical neck of the humerus and similar lesions. J Am Med Assoc 1949;141:1111-3.
3. Clare DJ, Hersh CK, Athanasiou K. Biomechanical fixation strength in surgical neck fractures of the proximal humerus. Proceedings of the 31st American Orthopaedic Association, Annual Residents' Conference; Sacramento, Calif; February 20, 1998.
4. Cornell CN, Levine D, Pagnani MJ. Internal fixation of proximal humerus fractures using the screw-tension band technique. J Orthop Trauma 1994;8:23-7.
5. Cuomo F, Flatow EL, Maday MG, et al. Open reduction and internal fixation of two- and three-part displaced surgical neck fractures of the proximal humerus. J Shoulder Elbow Surg 1992; 1:287-95.
6. Esser RD. Treatment of three- and four-part fractures of the proximal humerus with a modified cloverleaf plate. J Orthop Trauma 1994;8:15-22.
7. Gregory P, Sanders R. Compression plating versus intramedullary fixation of humeral shaft fractures. J Am Acad Orthop Surg 1997;5:215-23.
8. Hall MC, Rosser M. The structure of the upper end of the humerus with reference to osteoporotic changes in senescence leading to fractures. Can Med Assoc J 1963;88:290-4.
9. Hawkins RJ, Bell RH, Gurr K. The three-part fracture of the proximal part of the humerus: operative treatment. J Bone Joint Surg Am 1986;68:1410-4.
10. Inman VT, Saunders M, Abbott LC. Observations on the function of the shoulder joint. J Bone Joint Surg 1944;26:1-30.
11. Instrum K, Fennell C, Shrive N, et al. Semitubular blade plate fixation in proximal humeral fractures: a biomechanical study in a cadaveric model. J Shoulder Elbow Surg 1998;7:462-6.
12. Jaberg H, Warner JP, Jakob RP. Percutaneous stabilization of unstable fractures of the humerus. J Bone Joint Surg Am 1992; 74:508-15.
13. Koval KJ, Blair B, Takei R, Kummer FJ, Zuckerman KD. Surgical neck fractures of the proximal humerus: a laboratory evaluation of ten fixation techniques. J Trauma 1996;40:778-83.
14. Koval KJ, Sanders R, Zuckerman JD, et al. Modified-tension band wiring of displaced surgical neck fractures of the humerus. J Shoulder Elbow Surg 1993;2:85-92.
15. Kristiansen B, Christensian SW. Plate fixation of proximal humeral fractures. Acta Orthop Scand 1986;57:320-3.
16. Kristiansen B, Kofoed H. Transcutaneous reduction and external fixation of displaced fractures of the proximal humerus: a controlled clinical trial. J Bone Joint Surg Br 1988;70:821-4.
17. Liew ASL, Johnson JA, Patterson SD, et al. Effect of screw placement on fixation within the humeral head. J Shoulder Elbow Surg 2000;9:423-6.
18. McElhaney J, Fogle J, Byars E, Weaver G. Effect of embalming on the mechanical properties of beef bone. J Appl Physiol 1964; 19:1234-6.
19. Mouradian WH. Displaced proximal humeral fractures: seven years' experience with a modified Zickel supracondylar device. Clin Orthop 1986;212:209-18.
20. Muller ME, Allgower M, Schneider R, Willenegger H. Manual of internal fixation: techniques recommended by the AO group. 3rd ed. Berlin: Springer-Verlag; 1991. p. 438-41.
21. Naidu SH, Bixler B, Capo JT, Moulton JR, Radin A. Percutaneous pinning of proximal humerus fractures: a biomechanical study. Orthopedics 1997;20:1073-6.
22. Neer CS. Displaced proximal humeral fractures: part I. Classification and evaluation. J Bone Joint Surg Am 1970;52:1077-89.
23. Orthopaedic Trauma Association Fracture and Dislocation Compendium. Fracture and dislocation compendium. J Orthop Trauma 1996;10(Suppl 1):1-154.

24. Paavolainen P, Bjorkenheim JM, Slatis P, Paukku P. Operative treatment of severe proximal humerus fractures. Acta Orthop Scand 1983;54:374-9.
25. Poppen NK, Walker PS. Forces at the glenohumeral joint in abduction. Clin Orthop 1978;135:165-70.
26. Rajasekhar C, Ray PS, Bhamra MS. Fixation of proximal humeral fractures with the Polarus nail. J Shoulder Elbow Surg 2001;10: 7-10.
27. Ruch DS, Glisson RR, Marr WM, Russell GB, Nunley JA. Fixation of three-part proximal humeral fractures: a biomechanical evaluation. J Orthop Trauma 2000;14:36-40.
28. Sehr JR, Szabo RM. Semitubular blade plate for fixation in the proximal humerus. J Orthop Trauma 1988;2:327-32.
29. Sturzenegger M, Fornaro E, Jakob RP. Results of surgical treatment of multifragmented fractures of the humeral head. Arch Orthop Trauma Surg 1982;100:249-59.
30. Vesely DG. Use of the split diamond nail for fractures of the humerus. Clin Orthop 1985;41:145-56.
31. Wesley MS, Barenfield PA, Eisenstein AL. Rush pin intramedullary fixation for fractures of the proximal humerus. J Trauma 1977;17: 29-37.
32. Wheeler DL, Colville MR. Biomechanical comparison of intramedullary and percutaneous pin fixation for proximal humeral fracture fixation. J Orthop Trauma 1997;11:363-7.
33. Yamano Y. Comminuted fractures of the proximal humerus treated with hook plate. Arch Orthop Trauma Surg 1986;105:359-63.